*Journal of Applied Electrochemistry* **31**: 403–409, 2001.



# Theoretical and experimental studies of the dynamic behaviour of plug flow electrochemical reactors for a step change in flow rate

J.M. BISANG
*Programa de Electroquímica Aplicada e Ingeniería Electroquímica (PRELINE), Facultad de Ingeniería Química (UNL), Santiago del Estero 2829, 3000 Santa Fe, Argentina*

Received 4 July 2000; accepted in revised form 17 October 2000

*Key words:* dynamic behaviour, electrochemical engineering, flow rate perturbation, stability analysis

**Abstract**

This work presents an analysis of the dynamic behaviour of a plug flow electrochemical reactor for a step change in flow rate. The mathematical model takes into account the temporal variation of the mass transfer coefficient of the electrochemical reaction by means of an empirical expression with one parameter. To simplify the numerical solution of the general differential equation different assumptions are made. Thus, analytical equations of the transient current response are obtained. The theoretical treatments are compared with experimental results, obtained from copper deposition in a parallel-plate electrochemical reactor, in order to determine the reliability and the correlation capability of the mathematical models. The influence of the empirical parameter values on the performance of the reactor is also analysed.

**List of symbols**

$a_e$ specific surface area ($m^{-1}$)
$C$ concentration (mol $m^{-3}$)
$C_0$ inlet concentration (mol $m^{-3}$)
$F$ faradaic constant (A s $mol^{-1}$)
$g$ function given by Equation 26
$H$ Heaviside shifting function
$i$ current density (A $m^{-2}$)
$I$ total current (A)
$k$ mass transfer coefficient (m $s^{-1}$)
$k^*$ mass transfer coefficient before perturbation (m $s^{-1}$)
$k_s$ steady state mass transfer coefficient after perturbation (m $s^{-1}$)
$L$ electrode length (m)
$Q$ volumetric flow rate ($m^3$ $s^{-1}$)
$Q^*$ volumetric flow rate before perturbation ($m^3$ $s^{-1}$)
$s$ Laplace transform operator
$S$ cross-sectional area of the reactor ($m^2$)
$t$ time (s)
$u$ current per unit electrode volume (A $m^{-3}$)
$U$ Laplace transformed current per unit electrode volume
$v$ superficial liquid flow velocity (m $s^{-1}$)
$x$ axial coordinate (m)
$X$ normalized axial coordinate

*Greek characters*
$\alpha$ constant in Equation 12 (s)
$\beta$ constant given by Equation 28
$\beta^*$ constant given by Equation 6
$\epsilon$ porosity
$\phi$ function given by Equation 19
$\nu_e$ charge number of the electrode reaction
$\tau$ residence time after perturbation (s)
$\tau^*$ residence time before perturbation (s)

## 1. Introduction

Methods of predicting the dynamic behaviour of electrochemical reactors are of great interest in applied electrochemistry in order to determine the temporal response of the systems and to know the time required to reach the steady-state value. The dynamic behaviour of electrochemical reactors was summarized by Fahidy [1], Scott [2] and more recently in [3].

In a previous work from this laboratory [4] a mathematical model of predicting the dynamic behaviour of electrochemical reactors for a step change in flow rate when the kinetic constant is not a function of the flow rate has been developed. The predictions of the model are valid when the electrochemical reaction is charge transfer controlled or is under combined diffusion and charge transfer control for rotating electrodes, where the effect of the volumetric flow rate on the mass-transfer coefficient can be neglected. However, a new model suppressing the above assumptions is needed to take into account the dynamic behaviour of plug flow electrochemical reactors under conditions used in practice.

Thus, the mathematical model reported here assumes that the mass transfer coefficient varies with time according to an empirical expression with one parameter. The aim of this work is to compare the mathematical models with experimental results in order to determine the reliability of the different theoretical treatments.

## 2. Mathematical model

The dynamics of a plug flow reactor corresponds to a distributed parameter system. The mass balance gives

$$\epsilon \frac{\partial C(x,t)}{\partial t} = -v \frac{\partial C(x,t)}{\partial x} - \frac{i(x,t)a_e}{v_e F} \tag{1}$$

Adopting the following expression for the kinetics:

$$i(x,t) = v_e F\, k(t) C(x,t) \tag{2}$$

The kinetic constant $k$, assumed to be independent of the position in the reactor, approaches the mass transfer coefficient when the Damköhler number is high [4]. Defining

$$X = \frac{x}{L} \tag{3}$$

and the current per unit electrode volume as

$$u(X,t) = i(X,t)a_e \tag{4}$$

Combining Equations 1–4 and rearranging yields

$$\frac{\partial u(X,t)}{\partial t} - \frac{u(X,t)}{k(t)a_e}\frac{\mathrm{d}k(t)a_e}{\mathrm{d}t} = -\frac{1}{\tau}\frac{\partial u(X,t)}{\partial X} - \frac{k(t)a_e}{\epsilon}u(X,t) \tag{5}$$

with the following initial and boundary conditions:

$$t = 0 \quad u(X,0) = v_e F\, k^* a_e C_0 \exp(-\beta^* X) \quad \text{for all } X \tag{5a}$$

$$X = 0 \quad u(0,t) = v_e F\, k(t) a_e C_0 \quad \text{for all } t \tag{5b}$$

where

$$\beta^* = \frac{k^* a_e \tau^*}{\epsilon} \tag{6}$$

The total current is given by

$$I(t) = SL \int_0^1 u(X,t)\mathrm{d}X \tag{7}$$

To calculate the transient response in current, which represents the main difference with chemical reactors, it is necessary to know the variation of the mass transfer coefficient with time.

### 2.1. *Model assuming an empirical equation for $k(t)$*

Because of the complex nature of the hydrodynamics in an electrochemical reactor, it is difficult to predict the temporal variation of the mass transfer coefficient. However, $k(t)a_e$ must fulfil the following limiting conditions:
At $t = 0$

$$k(0)a_e = k^* a_e \tag{8}$$

and when the flow rate is increased

$$\left.\frac{\mathrm{d}k(t)a_e}{\mathrm{d}t}\right|_{t=0} > 0 \tag{9}$$

For $t \to \infty$

$$k(t \to \infty)a_e = k_s a_e \tag{10}$$

and

$$\left.\frac{\mathrm{d}k(t)a_e}{\mathrm{d}t}\right|_{t\to\infty} = 0 \tag{11}$$

The following empirical equation satisfies the limiting conditions given by Equations 8–11

$$k(t)a_e = \frac{k^* a_e \alpha + k_s a_e t}{\alpha + t} \tag{12}$$

Equation 12 will be used for the mathematical modelling.

Solving Equation 5 for the steady state case yields

$$u(X) = v_e F\, k a_e C_0 \exp\left(-\frac{k a_e \tau}{\epsilon} X\right) \tag{13}$$

Expanding the exponential function in a Maclaurin series and ignoring terms of second and higher order, Equation 13 approaches

$$u(X) = v_e F\, k a_e C_0 \left(1 - \frac{k a_e \tau}{\epsilon} X\right) \tag{14}$$

The first derivative of Equation 14 is

$$\frac{\mathrm{d}u(X)}{\mathrm{d}X} = -\frac{v_e F\, C_0 (k a_e)^2 \tau}{\epsilon} \tag{15}$$

Equation 15 does not depend on $X$. To simplify the mathematical solution of Equation 5 an additional assumption will be made. Thus, in the following, Equation 15 will be accepted as valid for all $t$. Introducing Equation 15, evaluated at $t = 0$, into Equation 5 yields

$$\frac{\mathrm{d}u(X,t)}{\mathrm{d}t}+\left(\frac{k(t)a_\mathrm{e}}{\epsilon}-\frac{1}{k(t)a_\mathrm{e}}\frac{\mathrm{d}k(t)a_\mathrm{e}}{\mathrm{d}t}\right)u(X,t)=\frac{v_\mathrm{e}FC_0}{\epsilon}(k^*a_\mathrm{e})^2 \tag{16}$$

Solving Equation 16 gives

$$u(X,t)=\exp[-\phi(t)]\left\{\frac{v_\mathrm{e}FC_0(k^*a_\mathrm{e})^2}{\epsilon}\int_0^t\exp[\phi(t)]\mathrm{d}t+\exp[\phi(0)]u(X,0)\right\} \tag{17}$$

where $u(X,0)$ is given by Equation 5(a).

Introducing Equation 17 into Equation 7, solving and rearranging yields

$$\frac{I(t)}{I(0)}=\exp[-\phi(t)]\times\left\{\frac{v_\mathrm{e}FC_0SL(k^*a_\mathrm{e})^2}{\epsilon I(0)}\int_0^t\exp[\phi(t)]\mathrm{d}t+\exp[\phi(0)]\right\} \tag{18}$$

where $\phi(t)$ is given by

$$\phi(t)=\frac{k_\mathrm{s}a_\mathrm{e}}{\epsilon}t-\frac{\alpha}{\epsilon}(k_\mathrm{s}a_\mathrm{e}-k^*a_\mathrm{e})\ln(\alpha+t)-\ln\left(\frac{k^*a_\mathrm{e}\alpha+k_\mathrm{s}a_\mathrm{e}t}{\alpha+t}\right) \tag{19}$$

The two first terms on the right hand side of Equation 19 can be neglected, thus

$$\exp[-\phi(t)]\cong\frac{k^*a_\mathrm{e}\alpha+k_\mathrm{s}a_\mathrm{e}t}{\alpha+t} \tag{20}$$

Introducing Equation 20 into Equation 18 and solving yields

$$\frac{I(t)}{I(0)}=\frac{k^*a_\mathrm{e}\alpha+k_\mathrm{s}a_\mathrm{e}t}{\alpha+t}\left[\frac{v_\mathrm{e}FC_0SL(k^*a_\mathrm{e})^2}{\epsilon I(0)}\left(\frac{t}{k_\mathrm{s}a_\mathrm{e}}+\alpha\frac{k_\mathrm{s}a_\mathrm{e}-k^*a_\mathrm{e}}{(k_\mathrm{s}a_\mathrm{e})^2}\ln\frac{k^*a_\mathrm{e}\alpha+k_\mathrm{s}a_\mathrm{e}t}{k^*a_\mathrm{e}\alpha}\right)+\frac{1}{k^*a_\mathrm{e}}\right] \tag{21}$$

Solving Equation 7 taking into account Equation 14 at $t=0$ yields

$$\frac{I(0)}{SL}=v_\mathrm{e}Fk^*a_\mathrm{e}C_0\left(1-\frac{k^*a_\mathrm{e}\tau^*}{2\epsilon}\right) \tag{22}$$

Introducing Equation 22 on the right hand side of Equation 21 and rearranging gives

$$\frac{I(t)}{I(0)}=\frac{k^*a_\mathrm{e}\alpha+k_\mathrm{s}a_\mathrm{e}t}{(\alpha+t)k^*a_\mathrm{e}}\left[\frac{(k^*a_\mathrm{e})^2}{\epsilon\left(1-\frac{k^*a_\mathrm{e}\tau^*}{2\epsilon}\right)}\times\left(\frac{t}{k_\mathrm{s}a_\mathrm{e}}+\alpha\frac{k_\mathrm{s}a_\mathrm{e}-k^*a_\mathrm{e}}{(k_\mathrm{s}a_\mathrm{e})^2}\ln\frac{k^*a_\mathrm{e}\alpha+k_\mathrm{s}a_\mathrm{e}t}{k^*a_\mathrm{e}\alpha}\right)+1\right] \tag{23}$$

At low $t$ values, the bracket in Equation 23 approaches unity. Thus, Equation 23 is simplified to

$$\frac{I(t)}{I(0)}=\frac{k^*a_\mathrm{e}\alpha+k_\mathrm{s}a_\mathrm{e}t}{(\alpha+t)k^*a_\mathrm{e}} \tag{24}$$

Equation 24 can be linearized to give

$$g(t)=\frac{\alpha}{t} \tag{25}$$

where

$$g(t)=\frac{I(0)}{I(t)-I(0)}\frac{k_\mathrm{s}a_\mathrm{e}-k^*a_\mathrm{e}}{k^*a_\mathrm{e}}-1 \tag{26}$$

Therefore the empirical parameter $\alpha$ in Equation 12 can be obtained from the slope of a plot of $g(t)$ as function $t^{-1}$ for low $t$ values.

### 2.2. *Model assuming a constant value for k after a perturbation in flow rate*

Equation 5 is simplified to

$$\tau\frac{\partial u(X,t)}{\partial t}=-\frac{\partial u(X,t)}{\partial X}-\beta u(X,t) \tag{27}$$

with the following initial and boundary conditions:

$$t=0\quad u(X,0)=v_\mathrm{e}F\,k^*a_\mathrm{e}C_0\exp(-\beta^*X)\quad\text{for all } X \tag{27a}$$

$$X=0\quad u(0,t)=v_\mathrm{e}F\,k_\mathrm{s}a_\mathrm{e}C_0\quad\text{for all } t \tag{27b}$$

where

$$\beta=\frac{k_\mathrm{s}a_\mathrm{e}\tau}{\epsilon} \tag{28}$$

Laplace transformation of Equation 27 gives

$$\frac{\mathrm{d}U(X,s)}{\mathrm{d}X}+(\tau s+\beta)U(X,s)=\tau u(X,0) \tag{29}$$

Solving Equation 29 gives

$$U(X,s)=\frac{v_\mathrm{e}F\,k^*a_\mathrm{e}C_0\tau}{\tau s+\beta-\beta^*}\exp(-\beta^*X)+v_\mathrm{e}FC_0\times\left(\frac{k_\mathrm{s}a_\mathrm{e}}{s}-\frac{k^*a_\mathrm{e}\tau}{\tau s+\beta-\beta^*}\right)\exp[-(\tau s+\beta)X] \tag{30}$$

Introducing Equation 30 into Equation 7 and integrating yields

$$I(s) = \frac{SLv_e F\, k^* a_e C_0 \tau}{(\tau s + \beta - \beta^*)\beta^*}[1 - \exp(-\beta^*)] + SLv_e FC_0\left(\frac{k_s a_e}{s} - \frac{k^* a_e \tau}{\tau s + \beta - \beta^*}\right) \times \frac{1}{\tau s + \beta}[1 - \exp(-(\tau s + \beta))] \quad (31)$$

Performing the Laplace transform inversion of Equation 31 and rearranging yields

$$I(t) = \frac{SLv_e FC_0 k^* a_e}{\beta^*}[1 - \exp(-\beta^*)]\exp\left(-\frac{\beta - \beta^*}{\tau}t\right) + \frac{SLv_e FC_0 k_s a_e}{\beta}\left[1 - \exp\left(-\frac{\beta t}{\tau}\right)\right] - \frac{SLv_e FC_0 k^* a_e}{\beta^*}\exp\left(-\frac{\beta t}{\tau}\right)\left[\exp\left(\frac{\beta^* t}{\tau}\right) - 1\right] + \left\{\begin{array}{l} -\frac{SLv_e FC_0 k_s a_e}{\beta}\left[\exp(-\beta) - \exp\left(-\frac{\beta t}{\tau}\right)\right] \\ +\frac{SLv_e FC_0 k^* a_e}{\beta^*}\exp\left(-\frac{\beta t}{\tau}\right)\left[\exp\left(\beta^*\left(\frac{t}{\tau} - 1\right)\right) - 1\right] \end{array}\right\} \times H(t - \tau) \quad (32)$$

with

$$H(t - \tau) = 0 \quad t < \tau \quad (32a)$$

$$H(t - \tau) = 1 \quad t \geqslant \tau \quad (32b)$$

Solving Equation 7 taking into account Equation 13 at $t = 0$ yields

$$I(0) = \frac{SLv_e Fk^* a_e C_0}{\beta^*}[1 - \exp(-\beta^*)] \quad (33)$$

Combining Equation 32 and 33 gives

$$\frac{I(t)}{I(0)} = \exp\left(-\frac{\beta - \beta^*}{\tau}t\right) + \left(\frac{\tau^*}{\tau}\right) \times \frac{1 - \exp\left(-\frac{\beta t}{\tau}\right)}{1 - \exp(-\beta^*)} - \left[\frac{\exp\left(-\frac{\beta t}{\tau}\right)}{1 - \exp(-\beta^*)}\right]\left[\exp\left(\frac{\beta^* t}{\tau}\right) - 1\right] + \left\{ -\frac{\tau^*/\tau}{1 - \exp(-\beta^*)}\left[\exp(-\beta) - \exp\left(-\frac{\beta t}{\tau}\right)\right] + \frac{\exp\left(-\frac{\beta t}{\tau}\right)}{1 - \exp(-\beta^*)}\left[\exp\left(\beta^*\left(\frac{t}{\tau} - 1\right)\right) - 1\right]\right\} \times H(t - \tau) \quad (34)$$

For $t < \tau$ Equation 34 is simplified to

$$\frac{I(t)}{I(0)} = \left(\frac{\tau^*}{\tau}\right) \times \frac{1 - \exp\left(-\beta\frac{t}{\tau}\right)}{1 - \exp(-\beta^*)} + \frac{\exp\left(-\beta\frac{t}{\tau}\right)}{1 - \exp(-\beta^*)}\left\{1 - \exp\left[\beta^*\left(\frac{t}{\tau} - 1\right)\right]\right\} \quad (35)$$

and for $t \geq \tau$ Equation 34 yields

$$\frac{I(t)}{I(0)} = \left(\frac{\tau^*}{\tau}\right) \times \frac{1 - \exp(-\beta)}{1 - \exp(-\beta^*)} \quad (36)$$

Equation 36 does not depend on $t$. Thus, according to this model a step perturbation in flow rate is felt immediately in the electrochemical reactor up to time instant $\tau$. A similar conclusion was given by Fahidy [1] for a step perturbation in current.

### 2.3. *Model assuming a constant value for k at all t*

This case was solved in previous work from this laboratory [4], giving

$$\frac{I(t)}{I(0)} = \left(\frac{\tau^*}{\tau}\right) \times \frac{1 - \exp\left(-\beta\frac{t}{\tau}\right)}{1 - \exp\left(-\beta\frac{\tau^*}{\tau}\right)} + \frac{\exp\left(-\beta\frac{t}{\tau}\right)}{1 - \exp\left(-\beta\frac{\tau^*}{\tau}\right)} \times \left\{1 - \exp\left[\beta\frac{\tau^*}{\tau}\left(\frac{t}{\tau} - 1\right)\right]\right\} \quad (37)$$

Equation 37 coincides with Equation 35 when $k_s = k^*$.

## 3. Experimental details

Figure 1 shows a general diagram of the experimental setup. All experiments were performed in an electrochemical reactor with vertical parallel plate electrodes. The reactor was made of acrylic material and both electrodes had the same dimensions, 200 mm wide and 600 mm long. To increase the mass transfer coefficient and to make it independent of the position in the reactor, the interelectrode gap, 13 mm, was completely filled with 16 sheets of plastic net, 0.4 mm thread diameter and 1.29 × 1.55 mm mesh size. The porosity of the stacked nets was 0.82. The small value of the aspect ratio (i.e., the ratio of electrode separation to electrode length) justifies the use of the plug-flow model for the reactor. The anode was a sheet of expanded titanium, 0.75 mm thick, coated with $RuO_2$. Copper-coated nickel was used as cathode.

The solution flowed from a thermostated tank (30 °C) to the lower part of the reactor, and was collected in another tank. It was not recycled so that the inlet copper concentration remained constant. The flow circuit system also included a rotameter, a needle valve, a globe valve and an electrolyte by pass provided with a ball valve and a holder for a perforated membrane. Preliminary experiments were performed in order to obtain the flow rate in the by pass as a function of the hole diameter in the membrane. Thus, changing the perfo-

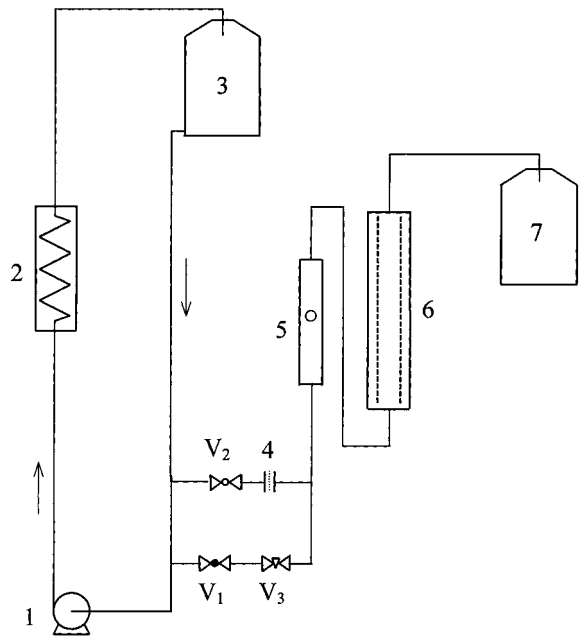


*Fig. 1.* Scheme of the electrolyte circulation system. Key: (1) pump, (2) thermostat, (3) thermostated tank, (4) holder for the perforated membrane, (5) flowmeter, (6) reactor, (7) reservoir, ($V_1$) globe valve, ($V_2$) ball valve and ($V_3$) needle valve.

rated membrane the magnitude of the step change in flow rate was controlled. The solution flow in the reactor was upwards and in order to achieve more uniform flow conditions along it, flow distributor plates with numerous small holes were arranged in the inlet and outlet regions. The same flow distributors were previously used [5] in a reactor with segmented counter electrode without plastic nets in the interelectrode gap and entrance effects were observed only in the first segment, approximately 2.5 cm. Likewise, Brown et al. [6] used plastic mesh promoters to help to reduce entrance effects near the inlet manifold. Therefore, in the present reactor the entrance length is negligible compared to the total electrode length.

The electrolyte solution was 1 M $Na_2SO_4$ and $H_2SO_4$, to obtain pH 2, with a copper concentration of approximately 1 g $l^{-1}$. The physical properties of the solution are given in Table 1 [3]. Therefore, the anodic reaction was oxygen evolution and copper deposition was the cathodic reaction. For each experiment the copper concentration was determined by iodimetry [7] with an accuracy of 0.7%.

All experiments were performed under potentiostatic control. The cathodic potential, controlled in the electrolyte inlet region, was −0.4 V against the saturated calomel electrode. This potential value was determined in a further experiment with a rotating disc electrode, where it was observed that at −0.4 V and over a potential range of 0.25 V the reaction is under limiting current condition and the hydrogen evolution is hindered. At the start of the experiment the ball valve denoted $V_2$ was closed and the electrolyte flowed by the circuit of valves denoted $V_1$ and $V_3$,

*Table 1.* Physical properties of the solution at 30 °C

| Property | Value |
|---|---|
| Kinematic viscosity | $1.11 \times 10^{-6}$ m$^2$ s$^{-1}$ |
| Density | $1.11 \times 10^{3}$ kg m$^{-3}$ |
| Diffusion coefficient | $5.16 \times 10^{-10}$ m$^2$ s$^{-1}$ |

when the steady state in current was achieved the valve $V_2$ was suddenly opened, so that a step change in the flow rate was produced, and the current was plotted as a function of time until a new steady state in current was achieved.

## 4. Results and discussion

Figure 2 shows the experimental values of $g(t)$ as a function of the inverse of time. The thin full lines correspond to the correlation of the data at low $t$ values according to Equation 25. Table 2 reports the values of $\alpha$ obtained from the slope of the lines in Figure 2. It can be seen that the $\alpha$ values are near to 10 s.

Figure 3 shows the experimental results, dotted lines, of the ratio between the current at time $t$ and the current before the perturbation as a function of time. The results of Equation 18 taking into account Equation 19, obtained by numerical integration, are given as the full line. The predictions of Equations 23 and 24 are also included. In all the theoretical calculations the $\alpha$ values given in Table 2 were used. The experimental results lie between the theoretical predictions of Equations 23 and 24. However, when the perturbation in flow rate is small the experimental data are close to the prediction of Equation 23 and they approach Equation 24 when the

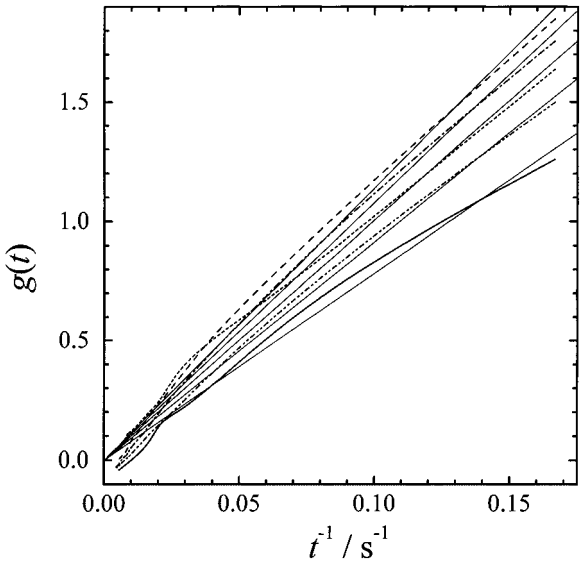


*Fig. 2.* $g(t)$ as a function of the inverse of time at various $Q/Q^*$ values: (——) 1.125, (- - - - -) 1.312, (· · · · ·) 1.381, (— · — · —) 1.617, (— · ·—) 1.886. $Q^* = 3.57 \times 10^{-6}$ m$^3$ s$^{-1}$. Thin full lines: correlation according to Equation 25 at low $t$ values.

perturbation in flow rate is higher. Likewise, the results of Equation 18 give the best agreement with the experimental data for the middle range of perturbation in flow rate.

Figure 4 compares the different mathematical models for the case reported in graph (d) of Figure 3. Thus, the curves in accordance with the Equations 35, 36 and 37 are also included. It can be observed that when the kinetic constant does not depend on the flow rate, curve (e), the dynamic behaviour is unimportant. Thus, the change in current is only produced for the concentration change inside the reactor. But when the change in flow rate produces a sudden change in the kinetic constant (case of Equation 35 represented by curve (d)), the transient response in current is more pronounced. Finally, when it is assumed that $k$ varies with time the electrochemical reactor achieves the new steady state at lower times than for the above case. Therefore, the comparison of curves (d) and (e) yields the effect of the variation of the kinetic constant with flow rate on the

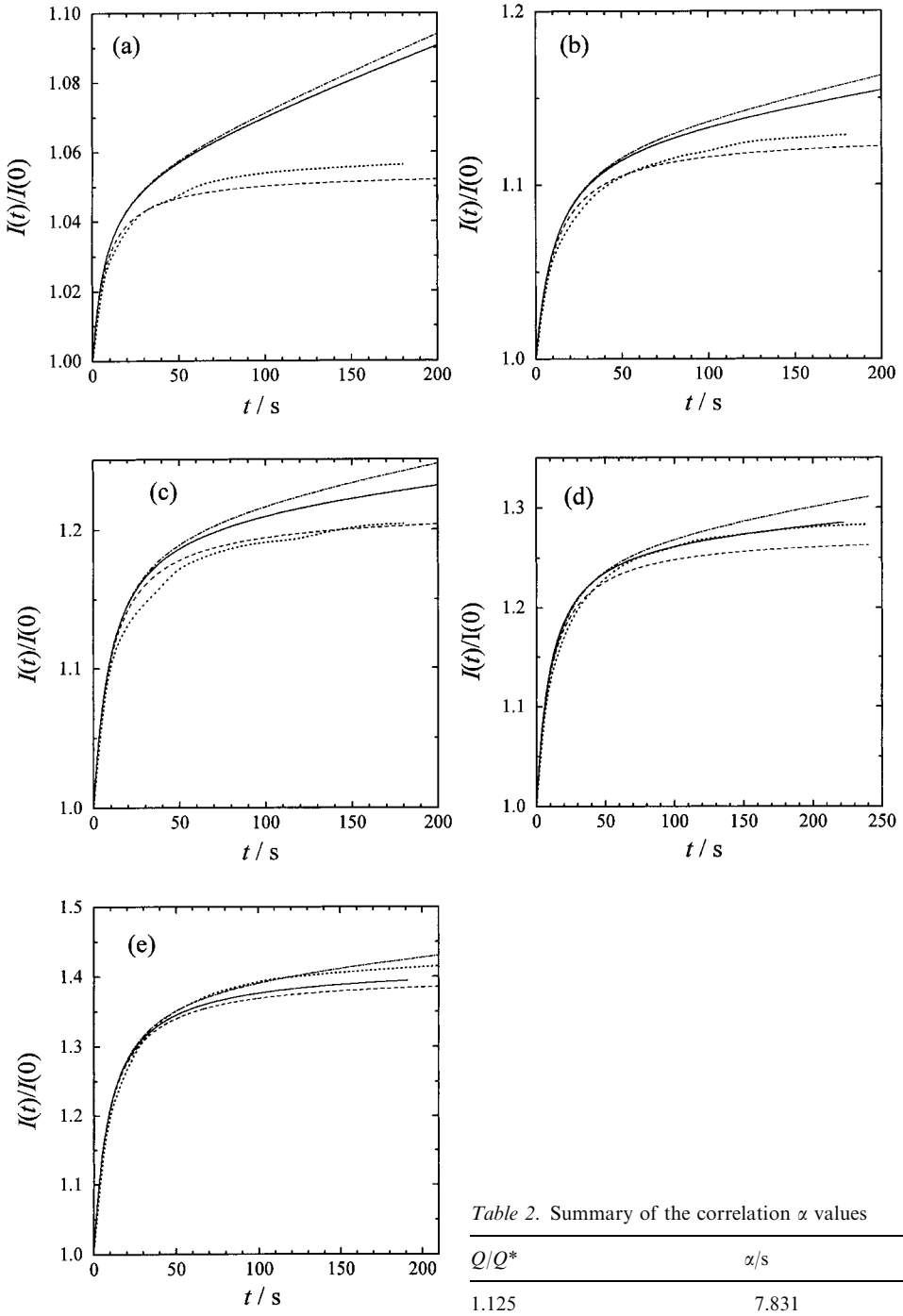


*Fig. 3.* Transient response in current. (a) $Q/Q^* = 1.125$, (b) 1.312, (c) 1.381, (d) 1.617 and (e) 1.886. $Q^* = 3.57 \times 10^{-6}\,m^3\,s^{-1}$. Key: (·····) experimental results, (——) Equation 18, (—·—·—) Equation 23 and (- - -) Equation 24.

*Table 2.* Summary of the correlation α values

| $Q/Q^*$ | α/s |
|---|---|
| 1.125 | 7.831 |
| 1.312 | 11.387 |
| 1.381 | 10.054 |
| 1.617 | 10.787 |
| 1.886 | 9.148 |

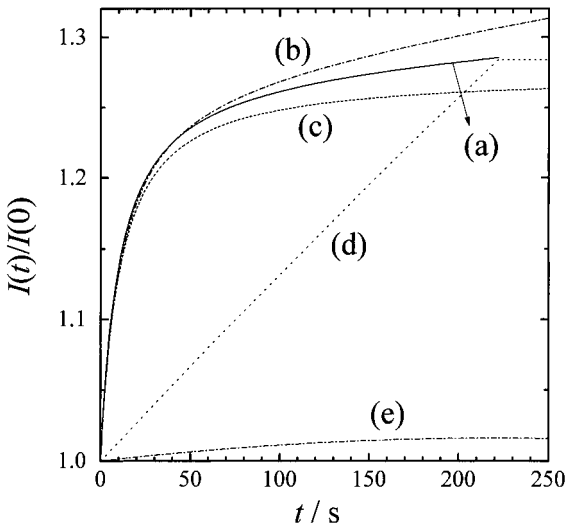


*Fig. 4*. Transient response in current according to different mathematical models. $Q/Q^* = 1.617$. $Q^* = 3.57 \times 10^{-6}\,m^3\,s^{-1}$. Key: (a) Equation 18, (b) Equation 23, (c) Equation 24, (d) Equations 35 and 36 and (e) Equation 37 with $k = k_s$.

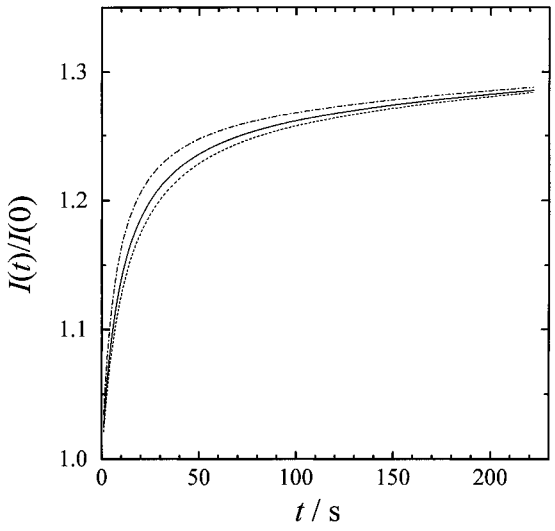


*Fig. 5*. Effect of $\alpha$ values on the transient response in current. $Q/Q^* = 1.617$. $Q^* = 3.57 \times 10^{-6}\,m^3\,s^{-1}$. Key: (——) $\alpha = 10$; (– · – · –) 7; (- - - -) 12.

transient behaviour in current. Likewise, the comparison between (a) and (d) curves gives the effect of the temporal variation of $k$.

To analyse the effect of $\alpha$ values on the dynamic behaviour, predictions according of Equation 18 are represented in Figure 5. It can be observed that all the curves are close. Thus the influence of $\alpha$ on the transient response of the electrochemical reactor is tolerable for engineering purposes when its value is in the range given in Table 2.

## 5. Conclusion

A mathematical model with an empirical expression for the temporal variation of the mass transfer coefficient is appropriate for correlation of experimental results. Thus, the reported theoretical treatment is a helpful tool to perform a simplified first analysis of the dynamic behaviour of plug flow electrochemical reactors.

## Acknowledgements

This work was supported by the Agencia Nacional de Promoción Científica y Tecnológica (ANPCyT), Consejo Nacional de Investigaciones Científicas y Técnicas (CONICET) and Universidad Nacional del Litoral (UNL) of Argentina.

## References

1. T.Z. Fahidy, 'Principles of Electrochemical Reactor Analysis', Elsevier, Amsterdam, (1985), Chapter 10, p. 244.
2. K. Scott, 'Electrochemical Reaction Engineering', Academic Press, London, (1991), Chapter 5, p. 318.
3. J.M. Bisang, *J. Appl. Electrochem.* **27** (1997) 379.
4. J.M. Bisang, *J. Appl. Electrochem.* **29** (1999) 1147.
5. J.M. Bisang, *J. Appl. Electrochem.* **23** (1993) 966.
6. C.J. Brown, D. Pletcher, F.C. Walsh, J.K. Hammond and D. Robinson, *J. Appl. Electrochem.* **22** (1992) 618.
7. W. Rieman and J.D. Neuss, 'Quantitative Analysis' (McGraw-Hill, New York, 1937), Chapter 15, p. 184.